2018 European Control Conference (ECC)
June 12-15, 2018. Limassol, Cyprus

Anticipative Robust Design Applied to a Water Level Control System

Asma Achnib[1,2], Tudor-Bogdan Airimitoaie[1], Patrick Lanusse[1], Ayadi Guefrachi[2], Mohamed Aoun[2], and Manel Chetoui[2]

***Abstract*— In this paper, a discrete-time robust controller design method for optimal reference tracking in preview systems is validated on an experimental test bench. In the context of preview systems, it is supposed that future values of the reference signal are available a number of time steps ahead. The objective is to design a control algorithm that minimizes a quadratic error between the reference and the output of the system. The proposed solution combines a robust feedback controller with a feedforward anticipative filter. The theoretical description of this new approach is given and experimental results on a water level control system are presented.**

***Index Terms*— anticipative control, robust control, feedforward filter, discrete-time systems**

I. INTRODUCTION

The concept of anticipative control (known also as preview control) was proposed initially in [19] and further developed in [21]. A complete review of anticipative control is presented in [11].

Anticipative control has been used in various automatic control applications namely in aeronautical systems [16], autonomous vehicles [20], mobile robots [5], water level control (for irrigation and drainage ducts in [18], [10]), etc. Furthermore, anticipative control has attracted the attention of many researches in other control areas and many works have been developed to combine other control techniques with anticipative action such as sliding mode control [23], multi-model adaptive control [22] and fuzzy control [3].

Recent research has focused on the design of the anticipative controllers in a $\mathscr{H}_2$ or $\mathscr{H}_\infty$ framework ([6], [13], [15], [14], [2]). Nevertheless, only a few number of research articles have attempted to deal with the problem of robust anticipative control. In [12], an anticipative control problem is considered in the context of motion control of robots. The proposed solution is also based on the $\mathscr{H}_\infty$ design methodology. Weighting norms are used to assure robustness of the feedback control law; however, uncertainties are not taken into account. In [11], a free-weighting matrices technique is used with Lyapunov stability theory to derive robust asymptotic stable anticipative controllers. Both reference anticipative tracking and disturbance rejection are treated but the proposed method based is dependant on the choice of the weighting matrices. In [1], a previously proposed method for designing GPC controllers is investigated. The method uses pre-defined closed-loop specifications of robustness and performance. In the absence of anticipation, the method shows satisfactory results. nevertheless, the analysis in an anticipative context shows that an equivalent anticipative feedforward filter appears whose design has to be taken into account to assure good tracking performances for the preview system.

The objective of the current paper is to validate a new approach for design of a discrete-time robust control methods with an anticipative action on an experimental test bench. It is based on a two degrees of freedom feedforward-feedback controller with anticipative reference filter. The anticipative feedforward filter with adjustable preview windows length is designed in the frequency domain using mixed $\mathscr{H}_2$ performance and $\mathscr{H}_\infty$ constraints for robustness with respect to plant model uncertainties. A CRONE (french acronym for Commande Robuste d'Ordre Non Entier, which translates to Fractional Order Robust Control) robust controller will be used for the feedback part. Throughout this paper, it is considered that future values of the reference signal are known a number of time steps ahead.

The paper is organised as follows. Notations used throughout the paper are introduced in Section II. The experimental test bench used for validation is described in Section III. The robust feedback controller designed using the CRONE methodology is given in Section IV and the proposed anticipative control solution is presented in Section V. Section VI discusses experimental results obtained on the test bench presented in Section III. Finally, SectionVII concludes this paper.

II. NOTATIONS

In this paper, signals are denoted with lower-case letters in the time domain and upper-case letters in the frequency domain. Transfer functions or polynomials are also denoted with upper-case letters. The unit delay operator q^{-1} is used in the time domain, while z^{-1} is used in the frequency domain. The unit advance operator q is used in the feedforward filters to represent the anticipative action. The sampling period is denoted by T_s, while the sampling frequency is represented by f_s.

As mentioned in the introduction, a feedforward–feedback discrete control structure for the reference tracking is studied and validate on an experimental test bench in this paper. A schematic representation of the controller is shown in Fig. 1.

*The work of Asma Achnib was supported by the Ministry of the Higher Education and Scientific Research in Tunisia.

[1]Univ. Bordeaux, Bordeaux INP, CNRS, IMS, UMR 5218, 33405 Talence, France `firstname.lastname@u-bordeaux.fr`

[2]University of Gabes, National Engineering School of Gabes, Tunisia, Research lab. Modeling, Analysis and Control of Systems (MACS) LR16ES22 `lastname.firstname@enig.u-gabes.tn`

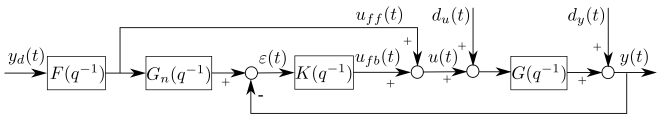

Fig. 1. Feedforward–feedback control schema used for robust anticipative control.

In Fig. 1, $G(q^{-1})$ represents the true plant model with uncertain parameters. It is supposed (without loss of generality) that the uncertainty intervals of the parameters are known. The true plant model can be considered as belonging to a set of models defined using the uncertainty intervals. The objective of robustness can be redefined as robustness to all the models in the model-set.

$G_n(q^{-1})$ denotes a nominal model chosen from the model set. The following factorisation is considered for the nominal model

$$G_n(q^{-1}) = G_h(q^{-1})G_l(q^{-1}), \tag{1}$$

where G_l includes the low frequency stable poles and minimum phase zeros of G_n. All the other poles and zeros of G_n are included in G_h. The difference between low and high frequency parts is based on the bandwidth of the system.

$G_n(q^{-1})$ functions as a pre-filter in Fig. 1 (if $G_n(q^{-1}) \equiv G(q^{-1})$ and $d_y(t) = 0$ then $\varepsilon(t) = 0$ and $u(t) = u_{ff}(t)$).

$K(q^{-1})$ is the robust feedback controller. $y_d(t)$, $u_{ff}(t)$, $u_{fb}(t)$, $u(t)$, $y(t)$, and $d(t)$ represent, respectively, the reference input, the feedforward control, the feedback control, the control input, the system output, and the disturbance signal.

$F(q^{-1})$ denotes the feedforward action for reference tracking.

Two closed-loop transfer functions in Fig. 1 are of interest:[1]

$$\frac{y(t)}{y_d(t)} = H_{yy_d}(q^{-1}) = GF\frac{1+KG_n}{1+KG} \tag{2}$$

gives the transfer from reference to system output, and

$$\frac{u(t)}{y_d(t)} = H_{uy_d}(q^{-1}) = F\frac{1+KG_n}{1+KG} \tag{3}$$

represents the transfer from reference to control input.

III. Description of the water tank test bench

The water level control part of a Festo didactic test bench has been used for the experimental validation (see Fig. 2). A schematic representation is given in Fig. 3. It is composed of:

- 2 pexiglass tanks (B101 used as water source and B102 used for the water level control);
- ultrasonic level indicator (LIC B101);
- manual valves (V102 and V110); and
- water pump (P101).

The valve V110 is partially open throughout the experiments presented in this paper.

The dynamic behaviour of the water level in the tank is non-linear as it depends on the water level. It is also uncertain as the valve V102 can be used in three positions: wide open, partially open and closed. For controller design, an identification of the test bench has been performed. A total of 18 first order continuous-time linear models have been obtained: 6 operating points for each one of the 3 positions of the V102 valve. Each operating point corresponds to a certain level of water in tank B102, going from 3 to 9 litres. The gains and time constants for the various models vary in the intervals: $k \in (0.118, 1.7)$ and $\tau \in (19.61, 205.8)$ (sec). The Bode diagrams of all the 18 models are shown in Fig.4.

[1]In some of the following equations, the parenthesis (q^{-1}) will be dropped to save space.

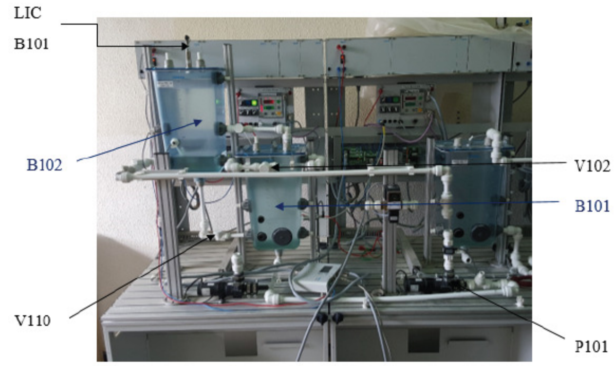

Fig. 2. Photo of the water level control test bench.

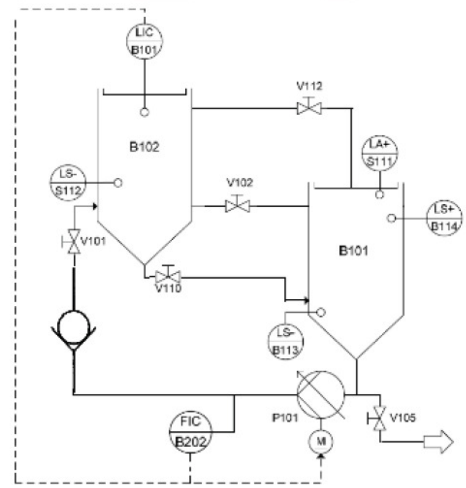

Fig. 3. Schema of the water level control test bench.

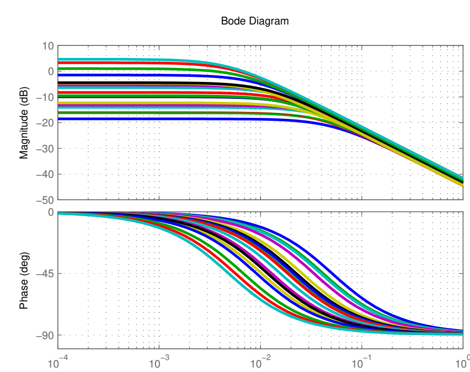

Fig. 4. Bode diagrams of all the 18 models.

An average nominal model is defined:

$$G_n(s) = \frac{0.332}{1+52.3169s}. \tag{4}$$

IV. Robust feedback CRONE controller design

In this section, the design of a linear robust controller K for the water level system using the CRONE methodology is presented. A discretization (z-transform taking into account a Zero Order Hold) of the continuous-time models, with sampling period T_s equals 1 sec, is performed. The Nichols chart of the uncertain model $G(q^{-1})$ is shown in Fig.5.

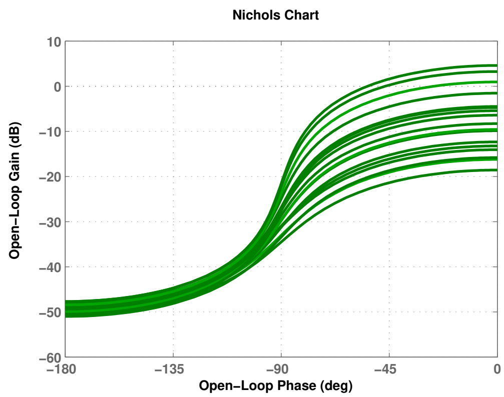

Fig. 5. Nichols chart of the uncertain parameters model $G(q^{-1})$.

The objective of the CRONE methodology is to robustify the closed-loop dynamic performance through a robust stability degree (robust resonant peak) and performance. The CRONE methodology uses fractional orders of integro-differentiator to make easier the controller robust design.

Looking at the Bode diagrams of the models for the various operation points, it can be noticed that large uncertainties occur in both magnitude and phase of the plant. The theoretical background for designing a third generation CRONE controller [17] for the given uncertain parameters plant is presented in this section; however, the computation of the controller's parameters is done using the CRONE Toolbox [8].

Let define the following sensitivity functions:

- Output sensitivity function
$$S(q^{-1}) = \frac{1}{1+G(q^{-1})K(q^{-1})}. \tag{5}$$
- Complementary sensitivity function
$$T(q^{-1}) = \frac{G(q^{-1})K(q^{-1})}{1+G(q^{-1})K(q^{-1})}. \tag{6}$$

In the previous equations, $G(q^{-1})$ can be any model from the model set. It is possible to define $S_n(q^{-1})$ and $T_n(q^{-1})$ if the nominal model $G_n(q^{-1})$ is used instead. For all other closed-loop sensitivity functions in Fig. 1, a composed notation is used (for example, $KS_n(q^{-1})$ denotes $K(q^{-1})S_n(q^{-1})$).

An aspect of CRONE design is that either continuous or pseudo-continuous transfer functions are used. As the objective is to find is a discrete robust controller, the discrete-time model set is transferred to the pseudo-continuous space using the W bilinear variable change.
$$q^{-1} = \frac{1-w}{1+w}$$
At the end, the inverse variable change will be used to get the discrete-time controller. Let us introduce the nominal open-loop transfer function
$$\beta_n(w) = G_n(w)K(w) = C_0\beta_l(w)\beta_m(w)\beta_h(w)\left(1-w\right), \tag{7}$$
$$\beta_l(w) = \left(\frac{v_0}{w}+1\right)^{n_l}, \quad \beta_h(w) = \frac{1}{\left(\frac{w}{v_1}+1\right)^{n_h}}, \tag{8}$$
$$\beta_m(w) = \left(\frac{1+w/v_1}{1+w/v_0}\right)^{a_0}\left(\Re_i\left\{\left(\alpha_0\frac{1+\frac{w}{v_1}}{1+\frac{w}{v_0}}\right)^{ib_{q_0}}\right\}\right)^{-q_0\mathrm{sign}(b_{q_0})} \tag{9}$$
with
$$\alpha_0 = \sqrt{\frac{1+\left(\frac{v_r}{v_0}\right)^2}{1+\left(\frac{v_r}{v_1}\right)^2}}. \tag{10}$$
w and v denote, respectively, the operational variable in the pseudo-continuous time domain and the pseudo frequency. Similarly to the continuous-time domain, $w = jv$. v is related to the frequency ω in continuous-time through $v = \tan(\frac{\omega T_s}{2})$.

- $(1-w)$ takes into account the right half plane zero of $G_n(w)$ in order to ensure the stability of the $KS(w)$ transfer function.
- $n_l = 1$ to ensure accuracy specifications at low frequencies.
- $n_h = 2$ to limit the high frequency control effort (decreasing transfer function $KS(w)$).
- a_0 and b_0 are the real and imaginary parts of the fractional order $a_0 + ib_0$ of band-limited integrator. v_0 and v_1 are their corner frequencies. The imaginary order b_{q_0} and the positive integer order q_0 are determined to ensure the same open-loop phase slope as the slope ensured by an initial imaginary order b_0 which may have to be limited for closed-loop stability reasons [9]. For large values of b_0, b_{q_0} is very close to b_0/q_0.
- From given values of the other parameters, a_0, b_{q_0}, q_0, and C_0 are deduced in order to ensure a resonant frequency v_r and a desired resonant peak M_{rd} of $|T_n(jv)|$. v_r and M_{rd} are used to tune the bandwidth and the damping of the nominal closed-loop transfer function $T_n(w)$.

The parameters of β_n are optimized together to stabilize the nominal closed-loop and to minimize the resonant peak variations of $T(w)$ at the time of the plant perturbation. The objective function to be minimized is defined by:
$$J_K = \sup_{v,G}|T(jv)| - M_{rd}. \tag{11}$$
Only 5 parameters of β_n need to be optimized: the v_0 and v_1 corner frequencies, the resonant frequency v_r, the resonant peak M_{rd}, $Y_r = |\beta_n(jv_r)|$. Setting the M_{rd} desired resonant peak for $|T_n(jv)|$ makes the Nichols plot of $\beta_n(jv)$ tangent to the M_{rd} Nichols M-contour. The minimization of J_K optimizes the tangency direction in order to place the perturbed open-loop frequency response $\beta(jv)$ away from the $(-\pi,\ 0\text{dB})$ critical point.

For the closed-loop performance requirement, a nonlinear minimization (using Matlab fmincon function) of J_K is carried out thanks to 5 sets of frequency-domain inequality constraints:
$$\inf_G|T(jv)| \geq T_l(v), \quad \sup_G|T(jv)| \leq T_u(v), \tag{12a}$$
$$\sup_G|S(jv)| \leq S_u(v), \tag{12b}$$
$$\sup_G|KS(jv)| \leq KS_u(v), \tag{12c}$$
$$\sup_G|GS(jv)| \leq GS_u(v). \tag{12d}$$

As the perturbations of G are taken into account without any overestimation (a set of LTI models), a non-conservative (highly efficient) robust controller can be designed. This modelling implies that a non-linear optimization method must be used to find the optimal values of the high-level descriptive parameters of fractional open-loop transfer function $\beta_n(w)$.

- $T_l(v)$ is defined by -1dB up to $v = 0.1$ for fast convergence and a good-enough bandwidth. Similarly, $T_u(v)$ is defined by $+1$ dB up to $v = 0.02$ for fast convergence. From 0.02 T_u is defined by 4.5 dB to avoid obtaining a very low stability degree.
- $S_u(v)$ has a $+20$ dB/dec slope at low frequency to desensitize the closed-loop system with respect to plant uncertainties and a value of 6 dB at high frequency to obtain a modulus margin greater than 0.5.
- $KS_u(v)$ has a value of 36 dB to limit the high frequency amplification of the measurement noise on the control input.
- $GS_u(v)$ has a $+20$ dB/dec slope at low frequency to ensure a good controller integral effect.

One obtains the following values for the optimal parameters: $v_0 = 0.0082, v_1 = 0.6$, $v_r = 0.1$, $M_{rd} = 1.74$ dB and $Y_r = 5.05$ dB. The deduced parameters are: $a_0 = 1.26, b_0 = \mathrm{b}_{q0} = 0.48, q_0 = 1$, and $C_0 = 12$. The value of the objective function $J_K = 0.35$ dB.

Once $\beta_n(w)$ has been optimized, the controller is obtained from

$$K(w) = G_n^{-1}(w)\beta_n(w). \tag{13}$$

As $\beta_n(w)$ is a fractional transfer function, an integer controller is obtained by identifying the ideal frequency response $K(jv)$ by a low-order transfer function

$$K_R(w) = \frac{K_N(w)}{K_D(w)}, \tag{14}$$

where $K_N(w)$ and $K_D(w)$ are polynomials of integer degrees n_{K_N} and n_{K_D}. Whatever the complexity of the control problem, the method presented in [17, Chapter 3] (see also [8]) — optimization of the zeros and poles of a given rational transfer function — enables small enough values of n_{K_N} and n_{K_D} to be used. For this example, $n_{K_N} = n_{K_D} = 4$. The discrete-time controller is obtained using the inverse of the bilinear variable change $w = \frac{1-q^{-1}}{1+q^{-1}}$.

The rational discrete-time controller is obtained as

$$K(q^{-1}) = \frac{22.97 - 40.89q^{-1} - 4.801q^{-2} - 40.9q^{-3} - 18.17q^{-4}}{1 - 2.973q^{-1} + 3.019q^{-2} - 1.119q^{-3} + 0.07266q^{-4}} \tag{15}$$

The constraints used for the sensitivity functions (see (12)) are given in Fig. 6 together with the obtained results. The maximum (minimum) response is obtained considering at each frequency the highest (lowest) value over the entire model set.

The Nichols chart of the obtained rational open-loop is compared to the fractional one in Fig. 7.

The linear closed loop time responses for the 18 operationg points are compared for a unit step reference in Fig. 8. The control input is also shown. Note that, during this simulation no saturation effects have been considered and no noise/disturbance have been added. The obtained results shows that the synthesized controller is rather robust to the plant perturbation.

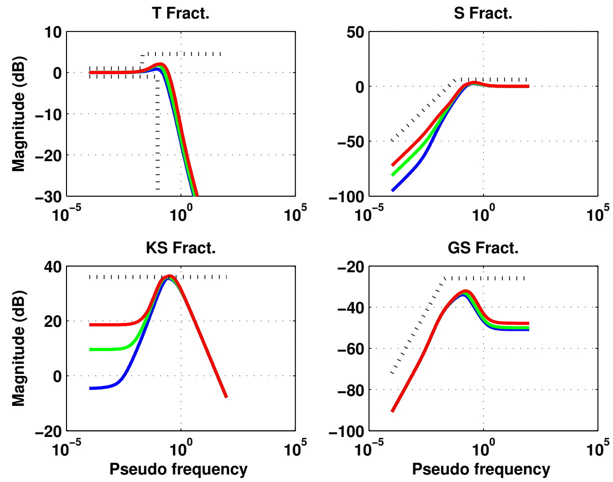

Fig. 6. Sensitivity functions templates and obtained results: green represents nominal open-loop, red is the highest response, and blue is the minimum response.

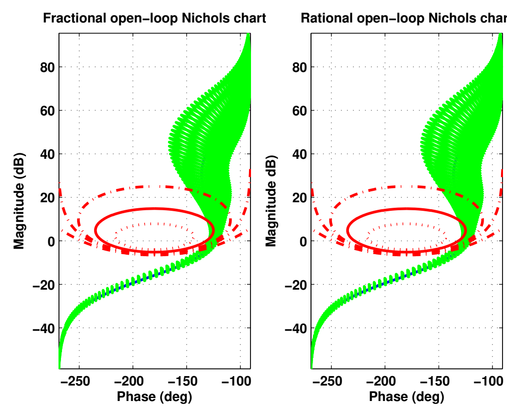

Fig. 7. Nichols comparison chart comparison between the fractional and the rational open-loop.

V. ANTICIPATIVE ROBUST DESIGN FOR REFERENCE TRACKING

In this section, the proposed design of the anticipative feedforward filters for the reference tracking is presented.

Let consider the following factorisation for the feedforward filter $F(q^{-1})$:

$$F(q^{-1}) = T_F(q^{-1})F_0(q^{-1}). \tag{16}$$

The F_0 factor in F is used to compensate the low frequency stable poles and minimum phase zeros of the plant G_n. F_0 is designed as the inverse of G_l: $F_0(q^{-1}) = G_l^{-1}(q^{-1})$. From (2), it can be seen that if $|KG| \gg 1$ and $|KG_n| \gg 1$ then H_{yy_d} tends to FG, which motivates the choice for F_0. $T_F(q^{-1})$ is an anticipative FIR filter:

$$T_F(q^{-1}) = t_{F_{-m}}q^{-m} + \ldots + t_{F_{-1}}q^{-1} + t_{F_0} + \\ + t_{F_1}q + \ldots + t_{F_a}q^a \ . \tag{17}$$

Remark: we chose a structure FIR because filter FIR allows anticipation and it is stable during optimization.

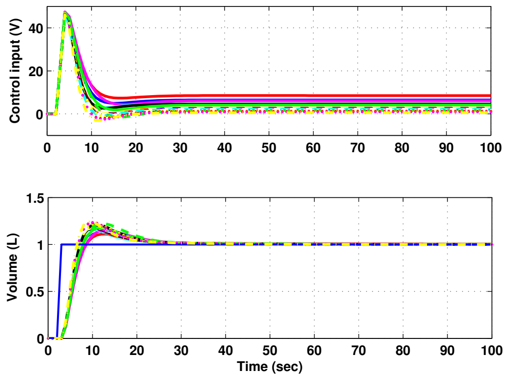

Fig. 8. Control effort and plant output of all the 18 models using the rational CRONE controller.

Due to $T_F(q^{-1})$, both past and future data are used when filtering a signal through $F(q^{-1})$. m represents the number of data that have to be saved in the *memory* of the filter. a gives the anticipation. A larger a means that information further in the future is needed. While the choice of m is limited only by the available memory, a has to be adjusted taking into account the time window of available future reference values. In practice, a and m have to be adjusted in accordance to the desired dynamics of the controlled system and the desired closed-loop response time.

Let denote

$$\theta_F = [t_{F_{-m}}, \ldots, t_{F_{-1}}, t_{F_0}, t_{F_1}, \ldots, t_{F_a}] \tag{18}$$

the vector of parameters of the unknown filter $T_F(q^{-1})$. In the rest of this section, the problem of finding the optimal estimation $\hat{\theta}_F$ is considered. The notations $T_F(\hat{\theta}_F, q^{-1})$ and $F(\hat{\theta}_F, q^{-1})$ correspond to $T_F(q^{-1})$ and $F(q^{-1})$ when $\hat{\theta}_F$ is used.

The previously defined closed-loop transfer functions (2) and (3) can be rewritten as:

$$\frac{y(t)}{y_d(t)} = H_{yy_d}(\theta_F, q^{-1}) = GF(\theta_F)\frac{1+KG_n}{1+KG} \tag{19}$$

$$\frac{u(t)}{y_d(t)} = H_{uy_d}(\theta_F, q^{-1}) = F(\theta_F)\frac{1+KG_n}{1+KG} \tag{20}$$

In order to minimize the ∞–norm of the error between the system output and the reference signal

$$\varepsilon_y(t) = y_d(t) - y(t) = (1 - H_{yy_d})y_d(t), \tag{21}$$

the following objective function is defined:

$$J_F(\theta_F) = \sup_t |\varepsilon_y(t)| = \sup_t \left|\left(1 - H_{yy_d}(\theta_F)\right) y_d(t)\right|. \tag{22}$$

For finite energy reference signals $y_d(t)$, a least upper bound of the previous objective functions can be obtained by using the $\mathscr{H}_2$ system norm[2] (see [4]).

$$J_F(\theta_F) \leq \left\|1 - H_{yy_d}(\theta_F, e^{-j2\pi f/f_s})\right\|_2 \|y_d(t)\|_2 \tag{23}$$

In this paper, the controller is designed off-line independently of the type and frequency content of the reference signal. As such, the $\mathscr{H}_2$ system norm in the previous equation is considered as optimization criterion of the anticipative feedforward filter

$$\hat{\theta}_F = \arg\min_{\theta_F} \left\|1 - H_{yy_d}(\theta_F, e^{-j2\pi f/f_s})\right\|_2, \tag{24a}$$

$$\text{s.t. } \lim_{q\to 1} T_F(\hat{\theta}_F, q^{-1}) = \lim_{q\to 1} {G_h}^{-1}(q^{-1}) \tag{24b}$$

$$\text{and } \left\|W_{uy_d}(e^{-j2\pi f/f_s}) H_{uy_d}(\hat{\theta}_F, e^{-j2\pi f/f_s})\right\|_\infty \leq 1 \tag{24c}$$

$$\forall f \in \left[0, \frac{f_s}{2}\right]$$

The constraint (24b) is introduced to ensure that the steady state gain of FG_n has unit value. The weighting function $W_{uy_d}(q^{-1})$ in (24c) introduces a frequency constraint on the control input u_{ff_F}. $W_{uy_d}(q^{-1})$ is chosen taking into account the characteristics of the plant that is controlled.

Robustness considerations in the design of the anticipative feedforward filter

The closed loop transfer functions $H_{yy_d}(\theta_F, q^{-1})$ and $H_{uy_d}(\hat{\theta}_F, q^{-1})$ that appear in the optimization problem (24) need the true plant model G for their computation. As this is not known exactly, it should be replaced by the models from the model-set. As such, (19) and (20) become:

$$H_{yy_d}(\theta_F, q^{-1}) = \\ = \left\{G_k \frac{1+KG_n}{1+KG_k} F(\hat{\theta}_F), \forall G_k \text{ in the model-set}\right\}, \tag{25}$$

and

$$H_{uy_d}(\hat{\theta}_F, q^{-1}) = \\ \left\{\frac{1+KG_n}{1+KG_k} F(\hat{\theta}_F), \forall G_k \text{in the model-set}\right\}. \tag{26}$$

(25) and (26) define two sets of transfer functions parametrized by the vector of parameters $\hat{\theta}_F$. The optimization problem (24) is redefined using (25) and (26) so that $\hat{\theta}_F$ should satisfy the criterion and the constraints for all H_{yy_d} and H_{uy_d} in the given sets.

Remark: in practice, it is possible to select only a smaller number of models from the model-set that contain the necessary information about the variations of the true plant for the design of the robust controller. The problem of how these models have to be selected is not dealt with in this paper. In Section VI, only the nominal model and two other models from the model-set are used.

VI. Experimental results

The approach presented in Section V is validated on the test bench described in Section III. The CRONE feedback controller presented in Section IV is used. For the computation of the feedforward filter, the Yalmip toolbox for Matlab is used with the MOSEK solver.

Throughout this section, it is considered that the disturbance $d(t)$ is equal to zero.

A. Anti-windup mechanism

In a number of experimental applications, the problem of actuator saturation persists. To deal with this problem an anti-windup mechanism is added to the controller. This anti-windup mechanism is based on an inner loop that feedbacks the integral part of the controller [7]. This is done by

[2]In the frequency domain, the q^{-1} operator becomes $e^{-j\omega T_s} = e^{-j2\pi f/f_s}$.

decomposing the discrete-time rational controller as

$$K(q^{-1}) = K_1(q^{-1}) + R_I \frac{1+q^{-1}}{1-q^{-1}} \tag{27}$$

where K_1 is without integral action.

The closed-loop control schema defined in Fig. 1 (without feedforward action for disturbance rejection) can be viewed in Fig. 9.

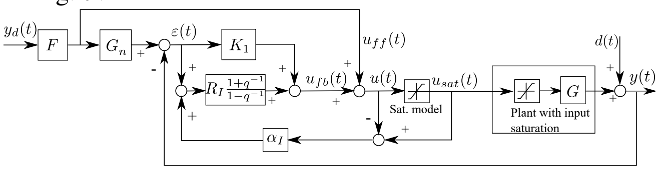

Fig. 9. Feedforward–feedback control schema used for robust anticipative control with anti-windup mechanism.

The gain α_I determines how quickly the integrator of the controller is reset. Remark that the bandwidth of the closed loop related to $\alpha_I R_I \frac{1+q^{-1}}{1-q^{-1}}$ is close to the bandwidth of the closed loop that includes K and G.

For the controller defined by (15), $R_I = 3.5084$, $\alpha_I = 1$ and

$$K_1(q^{-1}) = \\ = (1+q^{-1})\left[\frac{20.13}{1-0.08145q^{-1}} + \frac{0.7733}{1-0.8997q^{-1}} - \frac{1.439}{1-0.9915q^{-1}}\right].$$

The simulated control input and plant output (without feedforward) can be seen in Fig. 10.

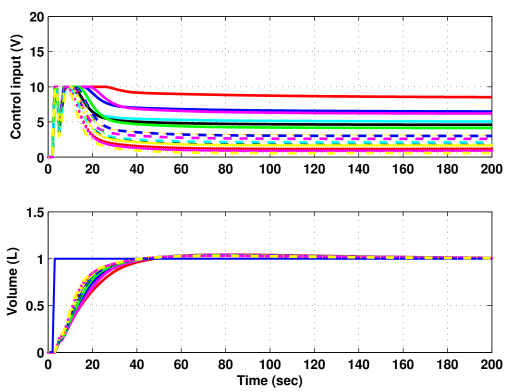

Fig. 10. Control effort and plant output of all the 18 models using the rational CRONE controller.

B. Evaluation of the proposed anticipative approach

An anticipative feedforward filter with 80 parameters has been computed. The anticipation introduced corresponds to a duration of 40 sec (order 40, sampling time $T_s = 1$ sec, $m = 39$ and $a = 40$). In all of the following figures, the green curve represents the result obtained with the nominal model G_n. Blue and red curves are the results for two other models from model set.

The discrete-time nominal model is obtained from (4) (z-transform and ZOH):

$$G_n(q^{-1}) = \frac{0.006286q^{-1}}{1-0.9811q^{-1}}. \tag{28}$$

The polynomials $G_h$and G_l^{-1} are given by

$$G_h(q^{-1}) = 0.006286q^{-1} \tag{29}$$

$$G_l^{-1}(q^{-1}) = 1 - 0.9811q^{-1} \tag{30}$$

The anticipative FIR filters $T_F(q^{-1})$ is obtained by solving the linear optimization problem (24)

$$T_F(q^{-1}) = 0.457q^{-39} + \ldots + 3.342 + \ldots + 0.4716q^{40} \tag{31}$$

As mentioned in Section V, $F_0(q^{-1}) = G_l^{-1}(q^{-1})$. A constraint of 6 dB has been imposed to control input sensitivity function above 0.1 rad/s. From Fig. 11 it can be seen that this constraint is globally satisfied for the three particular models of the plant.

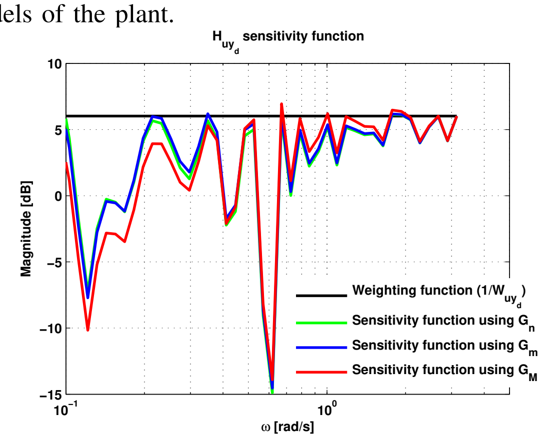

Fig. 11. Reference-control input sensitivity functions for nominal (green), minimum (blue) and maximum (red).

The feedforward anticipative filter in the presence of the CRONE controller described in Section IV has been implemented on the test bench described in Section III. Three configurations of the manual valve V102 are considered.

First the V102 valve is considered wide open. Experimental results are shown in Fig.12. Two step changes in the reference signal are tested. The first one is from 2 to 2.5 litres and the second from 2.5 to 3 litres. Good tracking results can be observed even in the presence of control input saturation (see Fig. 12).

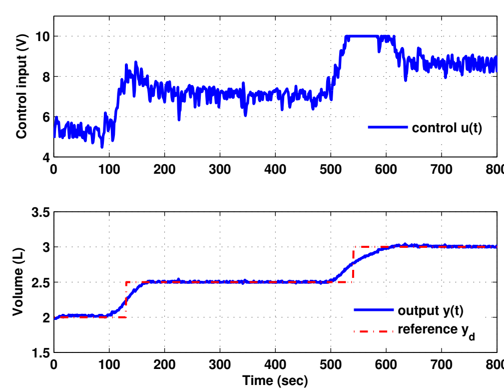

Fig. 12. Experimental results for the V102 manual valve wide open: control signal (upper plot), reference and output signals (lower plot).

In a second experiment, the V102 valve is considered only partially open. Experimental results are shown in Fig. 13. Due to the V102 valve being partially open, it is possible to track greater water volume reference signals. As such, in this experiment the reference varies from 2 to 4.5 litres by steps of 0.5 litres. As can be observed in Fig. 13, the output tracks the reference signal efficiently.

Finally, the V102 manual valve is completely closed. This allows to fill the water tank up to 8 litres. As before, step changes of 0.5 litres tests have been done; however, only two

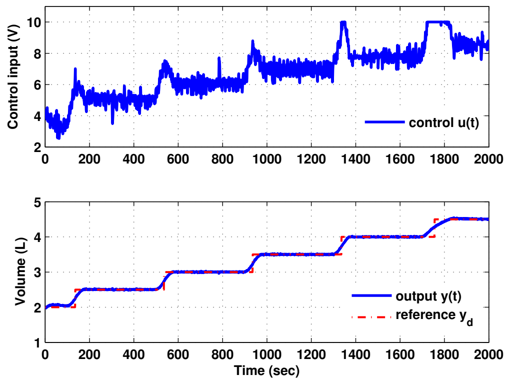

Fig. 13. Experimental results for the V102 manual valve partially open: control signal (upper plot), reference and output signals (lower plot).

of the step variations from 6 to 6.5 litres and from 6.5 to 7 litres are shown in Fig. 14.

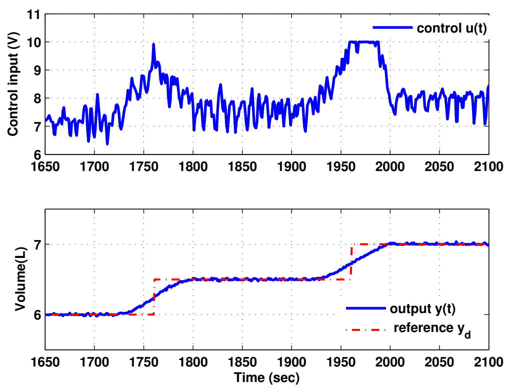

Fig. 14. Experimental results for the V102 manual valve completely closed: control signal (upper plot), reference and output signals (lower plot).

These experimental results show the robustness capabilities of the proposed approach. Despite significant changes in the plant frequency response for the various operation points and apertures of the V102 valve, and also the saturation of the control signal, the output of the system is efficiently tracking the desired reference trajectory.

Lastly, the anticipative effect of the feedforward filter is also noticeable in all experimental results. As expected, a 40 sec anticipation in introduced.

VII. CONCLUSIONS

In this paper, a recently developed approach for the control of preview systems is validated on an experimental water tank level control test bench. The design is based on the use of anticipative feedforward filters which are in the frequency domain using a mix of $\mathscr{H}_2$ performance and $\mathscr{H}_\infty$ constraints to ensure tracking of future references. The experimental results validate the robustness of the proposed approach in the case of reference tracking with respect to plant uncertainties.

In future work, this new approach will be extended to the case of multivariable systems.

REFERENCES

[1] Asma Achnib, Tudor-Bogdan Airimitoaie, Sergey Abrashov, and Patrick Lanusse. Generalized predictive controller performances in an anticipative context. In *2017 14th International Multi-Conference on Systems, Signals & Devices (SSD)*, 14th International Multi-Conference on Systems, Signals & Devices (SSD), Marrakech, France, March 2017. IEEE.

[2] Ahmad Akbari and Boris Lohmann. Output feedback H_∞ /GH_2 preview control of active vehicle suspensions: a comparison study of lqg preview. *Vehicle System Dynamics*, 48(12):1475–1494, 2010.

[3] JF Cheng, XX Dong, JP Xue, XP Wang, XF Wang, and JH Zhi. Fuzzy preview controller design for aircraft-pilot closed loop system. *Acta Aeronautica et Astronautica Sinica*, 35(3):807–820, 2014.

[4] John C Doyle, Bruce A Francis, and Allen R Tannenbaum. *Feedback control theory*. Macmillan Publishing Co., 1990.

[5] G. Freitas, F. Lizarralde, L. Hsu, and M. Bergerman. Terrain model-based anticipative control for articulated vehicles with low bandwidth actuators. In *Robotics and Automation (ICRA), 2013 IEEE International Conference on*, pages 382–389, May 2013.

[6] Akira Kojima and Shintaro Ishijima. H_∞ performance of preview control systems. *Automatica*, 39(4):693–701, 2003.

[7] P Lanusse, J Sabatier, and A Oustaloup. fractional order pid and first generation crone control system design. In *Fractional Order Differentiation and Robust Control Design*, pages 63–105. Springer, 2015.

[8] Patrick Lanusse. *CRONE Control System Design, a CRONE toolbox for Matlab*, 2010.

[9] Patrick Lanusse, Alain Oustaloup, and Valerie Pommier-Budinger. Stability of closed loop fractional order systems and definition of damping contours for the design of controllers. *International Journal of Bifurcation and Chaos*, 22(04):1230013, 2012.

[10] Y. Li. Offtake feedforward compensation for irrigation channels with distributed control. *IEEE Transactions on Control Systems Technology*, 22(5):1991–1998, Sept 2014.

[11] Fucheng Liao and Li Li. Robust preview tracking control for a class of uncertain discrete-time systems. *Cogent Engineering*, 3(1):1243033, 2016.

[12] Maria Makarov, Mathieu Grossard, Pedro Rodríguez-Ayerbe, and Didier Dumur. Modeling and preview H_∞ control design for motion control of elastic-joint robots with uncertainties. *IEEE Transactions on Industrial Electronics*, 63(10):6429–6438, 2016.

[13] Richard H Middleton, Jie Chen, and James S Freudenberg. Tracking sensitivity and achievable H_∞ performance in preview control. *Automatica*, 40(8):1297–1306, 2004.

[14] Agoes A Moelja and Gjerrit Meinsma. H2 control of preview systems. *Automatica*, 42(6):945–952, 2006.

[15] Antonio Moran Cardenas, Javier G Rázuri, Isis Bonet, Rahim Rahmani, and David Sundgren. Design of high accuracy tracking systems with H_∞ preview control. *Polibits*, 2014(50):21–28, 2014.

[16] Sanghyuk Park, John Deyst, and Jonathan How. A new nonlinear guidance logic for trajectory tracking. In *AIAA Guidance, Navigation, and Control Conference and Exhibit*. American Institute of Aeronautics and Astronautics, Aug 2004.

[17] Jocelyn Sabatier, Patrick Lanusse, Pierre Melchior, and Alain Oustaloup. *Fractional Order Differentiation and Robust Control Design*. Intelligent Systems, Control and Automation: Science and Engineering. Springer Netherlands, 2015.

[18] J. Schuurmans, A. Hof, S. Dijkstra, O. H. Bosgra, and R. Brouwer. Simple water level controller for irrigation and drainage canals. *Journal of Irrigation and Drainage Engineering*, 125(4):189–195, 1999.

[19] Thomas B Sheridan. Three models of preview control. *IEEE Transactions on Human Factors in Electronics*, HFE-7(2):91–102, 1966.

[20] Dong Hun Shin, Sanjiv Singh, and Ju Jang Lee. Explicit path tracking by autonomous vehicles. *Robotica*, 10(06):539–554, 1992.

[21] Masayoshi Tomizuka. Optimal continuous finite preview problem. *IEEE transactions on automatic control*, 20(3):362–365, 1975.

[22] Di Wang, Fucheng Liao, and Masayoshi Tomizuka. Adaptive preview control for piecewise discrete-time systems using multiple models. *Applied Mathematical Modelling*, 40(23):9932–9946, 2016.

[23] Markimba M Williams, Alexander G Loukianov, and Eduardo Bayro-Corrochano. Zmp based pattern generation for biped walking using optimal preview integral sliding mode control. In *Humanoid Robots (Humanoids), 2013 13th IEEE-RAS International Conference on*, pages 100–105. IEEE, 2013.